The Impact of the Layer Thickness on the Thermodynamic Properties of Pd Hydride Thin Film Electrodes

Paul Vermeulen,[†] Alexander Ledovskikh,[†] Dmitry Danilov,[‡] and Peter H. L. Notten*[,†,§]

Eindhoven University of Technology, 5600 MB Eindhoven, The Netherlands, Eurandom, 5600 MB Eindhoven, The Netherlands, and Philips Research Laboratories, 5656 AE Eindhoven, The Netherlands

Received: June 1, 2006; In Final Form: August 11, 2006

Recently, a lattice gas model was presented and successfully applied to simulate the absorption/desorption isotherms of various hydride-forming materials. The simulation results are expressed by parameters corresponding to several energy contributions, e.g., interaction energies. However, the use of a model system is indispensable in order to show the strength of the simulations. The palladium−hydrogen system is one of the most thoroughly described metal hydrides found in the literature and is therefore ideal for this purpose. The effects of decreasing the thickness of Pd thin films on the isotherms have been monitored experimentally and subsequently simulated. An excellent fit of the lattice gas model to the experimental data is found, and the corresponding parameters are used to describe several thermodynamic properties. It is analyzed that the contribution of H−H interaction energies to the total energy and the influence of the host lattice energy are significantly and systematically changing as a function of Pd thickness. Conclusively, it has been verified that the lattice gas model is a useful tool to analyze thermodynamic properties of hydrogen storage materials.

Introduction

Recently, a theoretical lattice gas model based on the principles of statistical thermodynamics has been proposed to calculate the thermodynamic properties of hydride-forming materials.[1] The model is able to describe the equilibrium electrode potentials and pressure-composition isotherms of metal hydrides (MH) as a function of hydrogen concentration in both the α and β solid solutions and two-phase coexistence region. In particular, equilibrium characteristics of $LaNi_yCu_{1.0}$ alloys with $4.0 \leq y \leq 5.0$ and Misch Metal-based AB_5 compounds at various temperatures were simulated. A good agreement between calculated and experimental isotherms was found.

However, the use of a so-called model system is indispensable to verify and ultimately show the strength of this model once more. Palladium hydride is ideal for this purpose, as it is one of the most thoroughly described metal−hydrogen systems found in the literature; e.g., a comprehensive monograph by Lewis is fully devoted to this system.[2] Moreover, extending the knowledge of PdH_x is desirable as, especially in thin film research aimed on developing high-energy density metal hydrides and switchable mirror materials, a thin Pd topcoat is often used to prevent the underlying layer from oxidizing.[3−6] Additionally, the Pd layer catalyzes H_2 dissociation in gas-phase loading and facilitates the charge-transfer process in electrochemical (de)hydrogenation.

In 1980, Frazier and Glosser reported a narrowing of the plateau width of isotherms of PdH_x layers as well as an increasing slope of the α-to-β phase-transition region with decreasing film thickness.[7] Extensive studies were carried out by Feenstra et al. also showed that the critical temperature (T_c) decreased as a function of film thickness.[8,9] While the former results were obtained from gas-phase experiments, Nicolas et al. used electrolytic (de)hydrogenation and showed the impact of the thickness of thin Pd layers (6−60 nm) with respect to T_c.[10] The marked drop of T_c with decreasing film thickness was attributed to clamping effects of the thin film to the substrate. More elaborate studies on the influence of the thickness of Pd films, within the range of 10−200 nm, on the isotherms and corresponding to thermodynamics have been performed and will be discussed in this contribution.

Experimental Methods

Palladium thin films, with a nominal thickness of 10, 50, 100, 150, and 200 nm, were deposited on thoroughly cleaned quartz substrates (diameter 20 mm) by means of electron beam deposition. A 10 Å thick Gd layer was deposited onto the substrate prior to Pd deposition to procure a good adhesion of Pd to the substrate. The pressure during deposition was between 1×10^{-7} and 1×10^{-6} mbar. Rutherford backscattering (RBS) was used to determine the film thickness. Electrochemical measurements were performed in a standard three-electrode setup. The potential of the Pd electrode, acting as the working electrode, was monitored versus a Hg/HgO reference electrode (Koslow Scientific Company, USA).[11] All measurements were performed in a strong alkaline environment (6 M KOH) and thermostated at 298 K. The experiments were carried out under a continuous Ar flow in order to deaerate the electrolyte, as it is known that even a small amount of O_2 can seriously affect, among other things, the hydrogen content as well as the electrochemical potential.[12] Galvanostatic intermittent titration technique (GITT) measurements were performed using an Autolab PGSTAT30 (Ecochemie B.V., The Netherlands). Unless stated otherwise, the cutoff voltage applied during the galvanostatic hydrogen extraction experiments was set to 0 V, and all electrochemical potentials are given versus Hg/HgO (6 M KOH).

Results and Discussion

In general, the electrochemical hydrogenation in an alkaline environment is described by two subsequent reactions. First,

* To whom correspondence should be addressed. E-mail: Peter.Notten@philips.com.
[†] Eindhoven University of Technology.
[‡] Eurandom.
[§] Philips Research Laboratories.

10.1021/jp063391y CCC: $33.50
Published on Web 09/08/2006

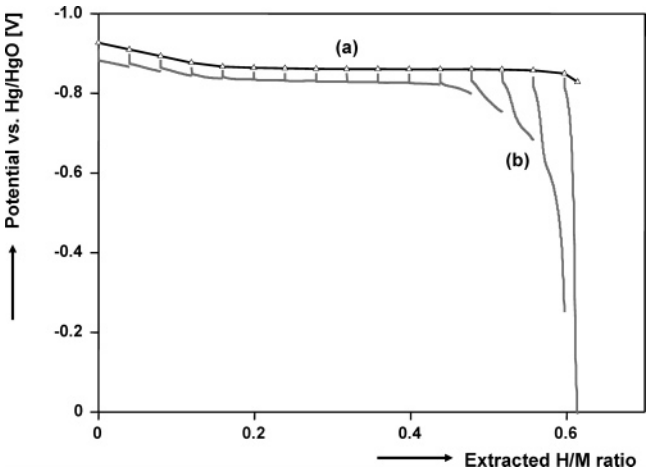

Figure 1. Equilibrium curve of a 150 nm thick Pd thin film electrode. The equilibrium points (Δ) are determined by means of GITT during discharging, and the corresponding isotherm is shown by curve (a). The electrochemical response during each current pulse (+0.12 mA) is shown by the gray curves (b).

H_2O is reduced at the metallic electrode (M) surface according to[13]

$$M + H_2O + e^- \rightleftarrows MH_{ad} + OH^- \quad (1)$$

Hereafter, the adsorbed H atom (H_{ad}) enters the metal and forms absorbed atomic hydrogen (H_{abs}) via

$$MH_{ad} \rightleftarrows MH_{ads} \quad (2)$$

During dehydrogenation, the reverse reactions take place. Unfortunately, there is a parasitic reaction where two H_{ad} atoms recombine to form molecular hydrogen gas, also known as the hydrogen evolution reaction (HER)

$$2MH_{ad} \rightleftarrows 2M + H_2\,(g) \quad (3)$$

The isotherms of Pd layers with various thicknesses were determined electrochemically. Generally, isotherms are obtained during hydrogenation, however, the HER can seriously intervene with the hydrogenation reaction, resulting in inaccurate hydrogen storage capacities. Therefore, to avoid the HER and to monitor the hydrogen content accurately, the electrochemically determined isotherms in this paper are measured during dehydrogenation.

The thin films were galvanostatically charged to their fully hydrogenated state using a current of −0.12 mA. Subsequently, the electrodes were allowed to equilibrate for 1 h. Hereafter, the PdH_x electrodes were discharged by means of GITT in approximately 20 pulses using a current of +0.12 mA. After each current pulse, the electrodes were allowed to equilibrate for 1 h. Figure 1 shows the experimentally determined equilibrium points (symbols), together with the corresponding equilibrium curve (black line), as well as the dynamic potential responses of a 150 nm thick Pd film during each current pulse (grey curves). From the latter, it is evident that during the hydrogen-rich β-solid solution and the β-to-α phase-transformation plateau, the overpotential (η) remains nearly constant, only to increase significantly at the hydrogen depleted state. In the electrochemical experiments, the ultrathin Gd adhesion layer is assumed not to influence the electrochemical response, as it is known from experiment that films of less than 3 monolayers do not absorb any appreciable amount of hydrogen.[14]

To simulate the thermodynamic properties of PdH_x, the recently developed lattice gas model is used.[1] Combining structural assumptions, mean field approximations and a binary alloy approach, the lattice gas model is able to describe the equilibrium potential of hydride-forming materials (E_{MH}^{eq}) as explicit functions of the normalized hydrogen concentration (x). A maximum of eight parameters is used to simulate and fit the experimental data. These parameters are the phase-transition points (x_α and x_β), the energies of the individual hydrogen atoms in their separate phases (E_α and E_β), the H−H interaction energies within the α and β phases ($U_{\alpha\alpha}$ and $U_{\beta\beta}$), the H−H interphase interaction energy between hydrogen atoms located in different phases ($U_{\alpha\beta}$), and finally, the energy of the host lattice (L), which corresponds to the energy of the unit cell of the hydride-forming material. Thus, according to the lattice gas model, the total description of E_{MH}^{eq} consists of three parts: the equilibrium potential of the α- (eq 4.1 below) and β-solid solutions (eq 4.3 below) and that of the two-phase coexistence region (eq 4.2 below), where $x_1 = (x - x_\alpha)/(x_\beta - x_\alpha)$, $x_2 = (x_\beta - x)/(x_\beta - x_\alpha)$, R is the gas constant, T the absolute temperature, and F is the Faraday constant. The entropy terms are defined as

$$S_\alpha^{\,0} = x_\alpha d \ln x_\alpha d + (1 - x_\alpha d)\ln(1 - x_\alpha d)$$
$$S_\beta^{\,0} = x_\beta \ln x_\beta + (1 - x_\beta)\ln(1 - x_\beta) \quad (5)$$

where d, the ratio between the number of host sites per unit cell in the α and β phase, was set to unity in all simulations.

To obtain a set of parameters with physical relevance, yielding continuous dependencies in eqs 4.1−4.3, some restrictions are imposed to the constants to preserve the continuity of the equilibrium potential at the phase-transition points (x_α and x_β), namely

$$\lim_{x\uparrow x_\alpha}(E_{MH}^{eq}(x)) = \lim_{x\downarrow x_\alpha}(E_{MH}^{eq}(x)) \text{ and } \lim_{x\uparrow x_\beta}(E_{MH}^{eq}(x)) = \lim_{x\downarrow x_\beta}(E_{MH}^{eq}(x)) \quad (6)$$

The experimental isotherms (symbols) of the extremes of the various Pd thicknesses (i.e., 10 and 200 nm) are plotted, as an example, as a function of the normalized hydrogen content together with the isotherms simulated by the lattice gas model

$$E_{MH}^{eq} = \frac{RT}{F}\begin{cases} \ln\left(\dfrac{1-xd}{xd}\right) - \dfrac{F}{RT}(E_\alpha + U_{\alpha\alpha}x), & 0 \le x < x_\alpha \quad (4.1) \\ \dfrac{\left(\dfrac{S_\alpha^{\,0}}{d} - S_\beta^{\,0}\right) - \dfrac{F}{RT}\left\{-E_\alpha x_\alpha - U_{\alpha\alpha}x_\alpha^{\,2}x_2 + E_\beta x_\beta + U_{\beta\beta}x_\beta^{\,2}x_1 + \dfrac{U_{\alpha\beta}x_\alpha x_\beta}{2}(x_2 - x_1) + L\right\}}{(x_\beta - x_\alpha)}, & x_\alpha \le x < x_\beta \quad (4.2) \\ \ln\left(\dfrac{1-x}{x}\right) - \dfrac{F}{RT}(E_\beta + U_{\beta\beta}x), & x \le x_\beta \quad (4.3) \end{cases}$$

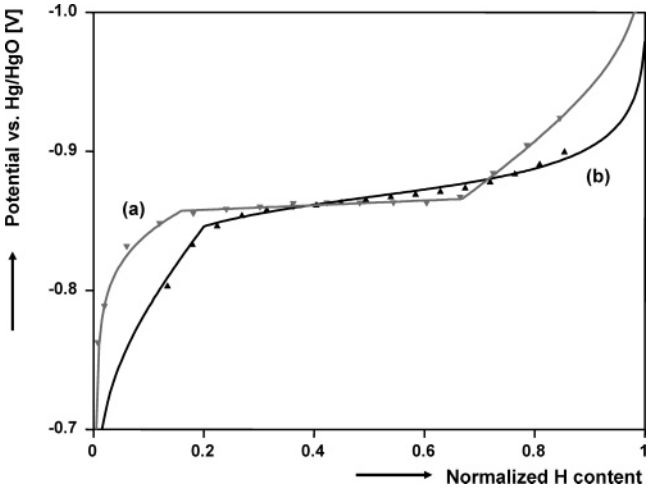

Figure 2. Measured (symbols) and calculated (lines) isotherms for 200 nm thick Pd (curve a) and 10 nm thick Pd electrode (curve b).

TABLE 1: Simulation Results for Pd Thin Films with a Thickness Ranging from 10 to 200 nm

Pd thickness (nm)	x_α	x_β	E_α [eV]	E_β [eV]	$U_{\alpha\alpha}$ [eV]	$U_{\beta\beta}$ [eV]	$U_{\alpha\beta}$ [eV]	L [eV]
10	0.196	0.196	−0.120	−0.038	0.366	−0.050		−0.008
50	0.130	0.370	−0.067	−0.065	0.312	0.001	0.126	0.006
100	0.140	0.473	−0.028	−0.093	0.008	0.059	0.176	0.017
150	0.149	0.600	−0.025	−0.139	0.0002	0.096	0.391	0.037
200	0.156	0.664	−0.034	−0.204	0.025	0.183	0.743	0.060

(solid lines) in Figure 2. As it is generally accepted to plot isotherms from low to high hydrogen content, it should be noted that the present dehydrogenation results are also plotted in this figure in accordance with this convention. First, the experimental data will be discussed in more detail. The isotherm of the 200 nm thick Pd thin film (curve a) shows a distinct and flat plateau at approximately −0.86 V, which is typical for bulk Pd. Contrastingly, the equilibrium curve of the 10 nm thick Pd electrode (curve b) shows a much more sloping plateau, which is an indication of the absence of a two-phase coexistence region. This observation is in line with results reported before that show that the critical temperature (T_c) is well below room temperature for very thin Pd films compared to 566 K for bulk Pd.[7−10,14]

More insight into the thermodynamic properties of palladium hydride as a function of its thickness can be obtained by analyzing the simulated parameter values that are listed in Table 1. Here, the most informative parameters are the interaction energies between hydrogen atoms in various phases ($U_{\alpha\alpha}$, $U_{\alpha\beta}$, $U_{\beta\beta}$) and the host energy contribution (L). The interaction energies within the α and β phases change into opposite directions with increasing film thickness. $U_{\alpha\alpha}$ declines, while $U_{\beta\beta}$ increases toward higher repulsion energies, i.e., more positive values. Nevertheless, the average values of the equilibrium potentials of both plateau regions are, however, very similar (see Figure 2). As the dependence of $U_{\alpha\alpha}$ and $U_{\beta\beta}$ with respect to the Pd thickness is found to be different, this difference should, therefore, in accordance with eqs 4.1−4.3, be compensated by the other parameters ($U_{\alpha\beta}$, L). From Table 1, it is evident that $U_{\alpha\beta}$ steadily increases as the thickness of the film increases, indicating a much stronger interphase interaction in the case of thick Pd layers compared to thinner films. Note that, for 10 nm thick Pd, no value for $U_{\alpha\beta}$ is given as the two-phase coexistence region was completely absent in this case.

There are two ways to explain the increase of $U_{\alpha\beta}$ as a function of film thickness: (i) As $U_{\alpha\alpha}$ and $U_{\beta\beta}$ clearly depend on the Pd thickness (Table 1), it is expected that the H−H interaction of H atoms located in different phases is also related to the film thickness. (ii) The variation of $U_{\alpha\beta}$ could also be related to the grain size of the α and β phases as for a small grain size, and as a consequence of large contact area between the phases and the fact that the lattice gas model is based on mean field theory, a stronger interaction is to be expected between the H atoms in separate phases. Therefore, $U_{\alpha\beta}$ will by definition increase in the case of a small grain size and implies that the grain size decreases as the Pd thickness increases. Research is currently in progress to verify if this is also found experimentally.

L also increases with increasing Pd thickness, and this may be attributed to the substrate. More specifically, in terms of the lattice gas model, L is defined as the transformation energy of the crystal lattice, and generally, this transformation is accompanied by a volume change of the unit cell. However, the Pd films discussed here are attached to a quartz substrate, and as a consequence, the rigid substrate causes resistance toward volume expansion. Therefore it is expected that the overall volume expansion, starting from the as-deposited state, is smaller in the case of Pd thin films comparing to bulk Pd, resulting in a decline of the host energy contribution. Overall, the large impact of the substrate on the thermodynamics of Pd thin films is in line with previous results.[7−10]

As the phase-transition points (x_α and x_β) are accurately determined using the mathematical model, it is possible to construct a phase diagram as a function of Pd thickness and normalized hydrogen content. This is depicted in Figure 3. The phase boundaries x_α and x_β converge smoothly toward a single phase-transition point as the thickness of the film decreases and indicates that below 10 nm Pd the miscibility gap completely vanishes.

According to our lattice gas model, the Gibbs free energy (G) of the hydrogen storage material expressed in eV/H atom can be determined according to eqs 7.1−7.3, below.[1] Here, the Gibbs free energies for the pure solid solutions are given by eqs 7.1 and 7.3 accordingly, while eq 7.2 corresponds to the two-phase coexistence region. Figure 4 shows the behavior of the Gibbs free energies for the 200 (A) and 50 nm (B) thick Pd layers. The dashed curves (a) correspond to the Gibbs free energies of the α-phase, while the solid curves (b) correspond to the β-phase. The black lines (c) represent the Gibbs free energies of the total system. From Figure 4, it is evident that the Gibbs free energies of the solid solutions are never below the energy of the total system. This observation is in line with

$$G = \begin{cases} \left(E_\alpha x + \dfrac{U_{\alpha\alpha}x^2}{2}\right) + \dfrac{RT}{Fd}[xd\ln(xd) + (1-xd)\ln(1-xd)], & 0 \le x < x_\alpha \quad (7.1) \\ \left(E_\alpha x_\alpha x_2 + \dfrac{U_{\alpha\alpha}x_\alpha{}^2 x_2{}^2}{2} + E_\beta x_\beta x_1 + \dfrac{U_{\beta\beta}x_\beta{}^2 x_1{}^2}{2} + \dfrac{U_{\alpha\beta}x_\alpha x_\beta x_1 x_2}{2} + Lx_1\right) + \dfrac{RT}{F}\left[\dfrac{S_\alpha{}^0 x_2}{d} + S_\beta{}^0 x_1\right], & x_\alpha \le x < x_\beta \quad (7.2) \\ \left(E_\beta x + \dfrac{U_{\beta\beta}x^2}{2}\right) + \dfrac{RT}{F}[x\ln(x) + (1-x)\ln(1-x)], & x \le x_\beta \quad (7.3) \end{cases}$$

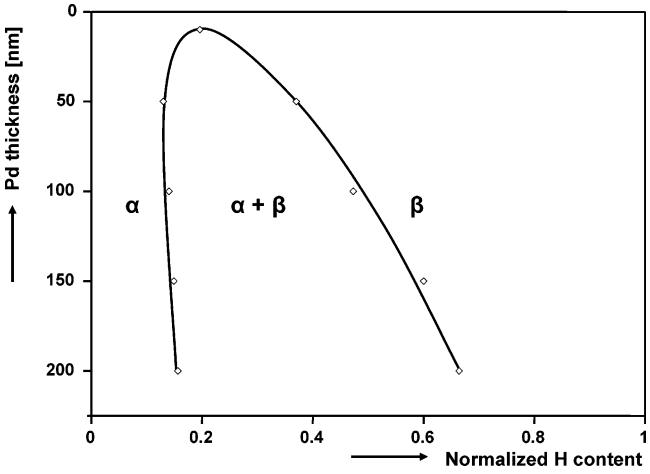

Figure 3. Calculated phase diagram vs the Pd electrode thickness.

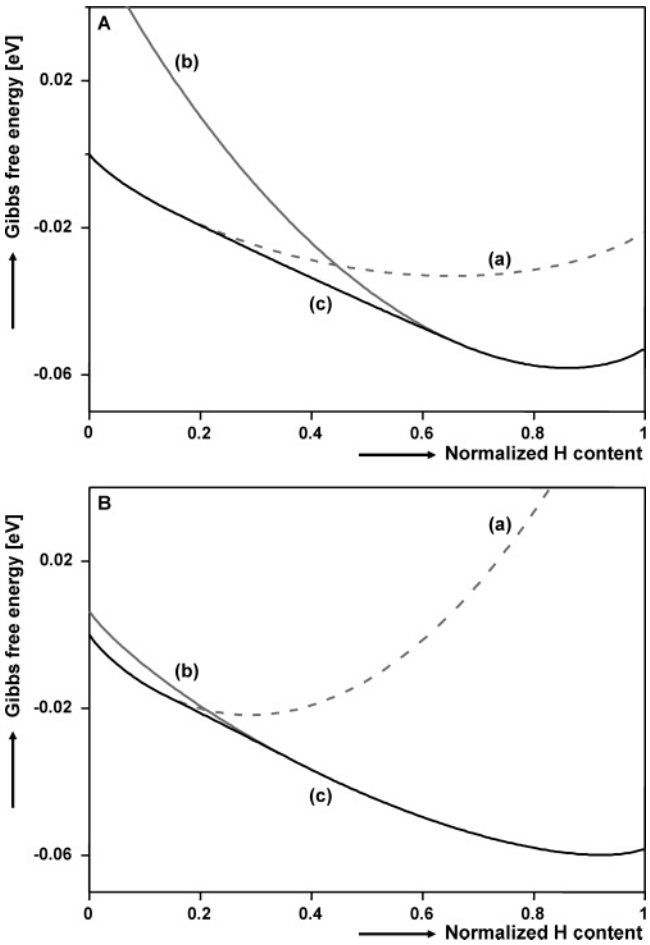

Figure 4. Evolution of the Gibbs free energy as a function of hydrogen content for Pd films with a nominal thickness of 200 nm (A) and 50 nm (B). The partial energy curves of the α-phase (a) and the β-phase (b) are shown together with the Gibbs free energy curves of the total system denoted by (c).

the principle of minimal energy, which states that the Gibbs free energy in the two-phase coexistence region is always lower than it can be for systems containing only one phase.

Furthermore, from Figure 4, it is apparent that for the 200 nm thick Pd film (A) the difference between the partial energies of the individual phases at the phase-transition points (x_α and x_β) is more pronounced compared to that of the thinner film (B). Therefore, the energy gain associated with the phase transition is relatively small for very thin Pd layers and is in accordance with the observation that the phase-transformation plateau is less apparent or even completely vanishes (see Figure 3).

Conclusions

The isotherms of Pd thin films with a nominal thickness of 10−200 nm are determined electrochemically and show that the isotherms change dramatically as a function of the layer thickness. For the 200 nm thick Pd electrode, a flat two-phase coexistence plateau is found, whereas for Pd films with a thickness of 10 nm, the transformation plateau has vanished, indicating the absence of a two-phase coexistence region. The lattice gas model is used to simulate the isotherms of PdH_x electrodes and to gain more insight into the correspondence to thermodynamics. The model parameters reveal a systematic change of the thermodynamic properties as a function of Pd thickness. In particular, closely analyzing the energy parameters reveals that the interphase interaction increases as a function of Pd thickness, which could be due to a relatively small grain size for thick Pd films. Moreover, it is shown that the influence of the substrate has a large impact, especially on the thinnest films. The phase diagram of Pd layers as a function its thickness reveals that the miscibility gap completely vanishes below 10 nm. This corresponds to the fact that the energy gain resulting from the phase transition is less in the very thin films. Finally, the successful application of the lattice gas model to the palladium−hydrogen system illustrates that the model is an excellent tool to determine the thermodynamic properties of hydrogen storage materials.

Acknowledgment. We very much appreciate the instructive and helpful remarks of our colleagues within the Electrochemical Energy Storage Group of the Department of Inorganic Chemistry and Catalysis at the Eindhoven University of Technology. We would like to thank T. Dao for the RBS results. Furthermore, financial support from the NWO ACTS Sustainable Hydrogen Program is acknowledged.

References and Notes

(1) Ledovskikh, A.; Danilov, D.; Rey, W. J. J.; Notten, P. H. L. *Phys. Rev. B* **2006**, *73*, 014106.
(2) Lewis, F. A. *The Palladium Hydrogen System*; Academic Press: London, 1967.
(3) Kremers, M.; Koeman, N. J.; Griessen, R.; Notten, P. H. L.; Tolboom, R.; Kelly, P. J.; Duine, P. A. *Phys. Rev. B* **1998**, *57*, 4943.
(4) Richardson, T. J.; Slack, J. L.; Armitage, R. D.; Kostecki, R.; Farangis, B.; Rubin, M. D. *Appl. Phys. Lett.* **1999**, *78*, 3047.
(5) Niessen, R. A. H.; Notten, P. H. L. *Electrochem. Solid-State Lett.* **2005**, *8*, A534.
(6) Borsa D. M.; Baldi, A.; Pasturel, M.; Schreuders, H.; Dam, B.; Griessen, R.; Vermeulen, P.; Notten, P. H. L. *Appl. Phys. Lett.* **2006**, *88*, 241910.
(7) Frazier, G. A.; Glosser, R. *J. Less-Common Met.* **1980**, *74*, 89.
(8) Feenstra, R.; de Bruin-Hordijk, G. J.; Bakker, H. L. M.; Griessen, R.; de Groot, D. G. *J. Phys. F: Met. Phys.* **1983**, *13*, L13.
(9) Feenstra, R.; de Groot, D. G.; Rector, J. H.; Salomons, E.; Griessen, R. *J. Phys. F: Met. Phys.* **1986**, *16*, 1953.
(10) Nicolas, M.; Dumoulin, L.; Burger, J. P. *J. Appl. Phys.* **1986**, *60*, 3125.
(11) Niessen, R. A. H.; Notten, P. H. L. *J. Electrochem. Soc.* **2005**, *152*, A2051.
(12) Niessen, R. A. H.; Notten, P. H. L. *Electrochim. Acta* **2005**, *50*, 2959.
(13) Notten P. H. L. Rechargeable Nickel−Metalhydride Batteries: A Successful New Concept. In *Interstitial Intermetallic Alloys*; Grandjean, F., Long, G. L., Buschow, K. H. J., Eds; Kluwer Academic Publishers: Dordrecht, 1995; NATO ASI Series E, Vol. 281, pp 151−195.
(14) de Ribaupierre, Y.; Manchester, F. D. *J. Phys. C: Solid State Phys.* **1974,** *7*, 2126.